JOURNAL OF VIROLOGY, Aug. 2010, p. 8062–8071 Vol. 84, No. 16
0022-538X/10/$12.00 doi:10.1128/JVI.00722-10

A Nine-Segment Influenza A Virus Carrying Subtype H1 and H3 Hemagglutinins▽†

Qinshan Gao,[1] Anice C. Lowen,[1] Taia T. Wang,[1] and Peter Palese[1,2]*

Departments of Microbiology[1] and Medicine,[2] Mount Sinai School of Medicine, New York, New York 10029

Received 5 April 2010/Accepted 25 May 2010

Influenza virus genomic RNAs possess segment-specific packaging signals that include both noncoding regions (NCRs) and adjacent terminal coding region sequences. Using reverse genetics, an A/Puerto Rico/8/34 (A/PR/8/34) virus was rescued that contained a modified PB1 gene such that the PB1 packaging sequences were exchanged for those of the neuraminidase (NA) gene segment. To accomplish this, the PB1 open reading frame, in which the terminal packaging signals were inactivated by serial synonymous mutations, was flanked by the NA segment-specific packaging sequences including the NCRs and the coding region packaging signals. Next, the ATGs located on the 3′ end of the NA packaging sequences of the resulting PB1 chimeric segment were mutated to allow for correct translation of the full-length PB1 protein. The virus containing this chimeric PB1 segment was viable and able to stably carry a ninth, green fluorescent protein (GFP), segment flanked by PB1 packaging signals. Utilizing this method, we successfully generated an influenza virus that contained the genes coding for both the H1 hemagglutinin (HA) from A/PR/8/34 and the H3 HA from A/Hong Kong/1/68 (A/HK/1/68); both subtypes of HA protein were also incorporated into the viral envelope. Immunization of mice with this recombinant virus conferred complete protection from lethal challenge with recombinant A/PR/8/34 virus and with X31 virus that expresses the A/HK/1/68 HA and NA. Using the described methodology, we show that a ninth segment can also be incorporated by manipulation of the PB2 or PA segment-specific packaging signals. This approach offers a means of generating a bivalent influenza virus vaccine.

Influenza viruses possess segmented, negative-sense RNA genomes and belong to the family of *Orthomyxoviridae*. Three types of influenza viruses have been identified: A, B, and C (24). Based on the two surface glycoproteins hemagglutinin (HA) and neuraminidase (NA), type A viruses are further divided into different subtypes; there are now 16 HA subtypes (H1 to H16) and 9 NA subtypes (N1 to N9) of influenza A viruses (24). Current influenza A viruses circulating in humans include the H1N1 and H3N2 subtypes.

The genomes of influenza A and B viruses consist of eight RNAs, while C viruses have only seven segments. Influenza virus genomic RNAs associate with nucleoprotein (NP) and three viral polymerase subunits (PB2, PB1, and PA), to form the ribonucleoprotein (RNP) complexes within virions (24). Previous data indicated that each segment of the influenza A/WSN/33 (H1N1) virus possesses segment-specific RNA packaging signals that include both the 3′ and 5′ noncoding regions (NCRs), as well as coding sequences at the two ends of each open reading frame (ORF) (4, 5, 10, 11, 13, 15, 22, 23, 28; and see Fig. 47.23 in reference 24). In addition, an electron microscopy study showed that the wild-type influenza A virus contains exactly eight RNPs within the virions, with seven RNPs surrounding a central one (19). These results suggest that influenza virus genome packaging is a specific process, with each particle containing eight unique RNA segments. Additional evidence supporting a specific packaging theory came from studies of defective interfering (DI) RNAs which contain internal deletions in the coding sequences. These short RNAs can be incorporated into the virus particles despite the fact that they do not encode full-length functional proteins. The finding that incorporation of DI RNAs interferes with the parent full-length RNAs in a segment-specific manner (1, 16, 17) also suggests that influenza virus genome packaging is a specific process.

However, there are also data arguing that influenza virus RNA packaging can be nonspecific. First, studies showed that the two different RNA segments of influenza virus can be engineered to share the same set of 3′ and 5′ NCRs, which are important components of the influenza virus RNA packaging signals (18, 31). In addition, under specific circumstances, influenza virus is able to contain nine RNA segments, in which two of them share identical NCRs and partially identical coding region sequences (2, 29). Titrations of the nine-segment virus revealed a linear relationship between dilutions and plaque numbers, suggesting an influenza virus virion can incorporate more than eight segments (2).

Herein, we describe a novel approach for the generation of nine-segment influenza viruses based on the manipulation of the segment-specific packaging signals. When the packaging sequences of the PB1 (or PB2 or PA) segment were replaced by those of the NA segment, influenza A/PR/8/34 virus was able to stably incorporate a ninth segment flanked by the PB1 (or PB2 or PA) packaging signals. Using this property, we successfully generated influenza viruses encoding two full-length HA glycoproteins: a subtype H1 A/PR/8/34 HA and a subtype H3 A/HK/1/68 HA. Immunization of mice with the virus carrying two HAs protected them from the lethal chal-

* Corresponding author. Mailing address: Department of Microbiology, Mount Sinai School of Medicine, Box 1124, One Gustave L. Levy Place, New York, NY 10029. Phone: (212) 241-7318. Fax: (212) 534-1684. E-mail: peter.palese@mssm.edu.

† Supplemental material for this article may be found at http://jvi.asm.org/.

▽ Published ahead of print on 2 June 2010.

lenge with either A/PR/8/34 or X31 virus, the latter of which carries the HA and NA genes of A/HK/1/68. This approach can be used to construct live attenuated influenza vaccine viruses targeting two heterologous strains.

MATERIALS AND METHODS

Cells and viruses. 293T cells were maintained in Dulbecco's modified Eagle's medium with 10% fetal calf serum (FCS). MDCK cells were grown in Eagle's minimal essential medium with 10% FCS. Viruses were grown in 10-day-old specific-pathogen-free chicken embryos at 37°C (Charles River Laboratories, SPAFAS).

Plasmid construction. (i) Generation of NA-PB1mut-NA, NA-PB2mut-NA, and NA-PAmut-NA constructs. The NA-PB1mut-NA, NA-PB2mut-NA, and NA-PAmut-NA constructs were generated as shown in Fig. 1A (left). To introduce silent mutations at the two ends of each ORF, the ORFs of the PB1, PB2, and PA genes were amplified by PCR from previously constructed pDZ-PB1, PB2, and PA constructs (25) and cloned into a pGEM-T vector (Promega). Forward primer 5′-CAGCTAGCATGGA**C**GT**T**AA**C**CC**A**AC**T**CT**G**T**T**ATT**T**C T**G**AA**G**GTA**C**C**G**GC**G**CA**G**AA**C**GC**C**AT**C**AG**T**AC**G**ACCTT**T**CCTTATACT GGAGAC-3′ and reverse primer 5′-GTCTCGAGCTA**C**TT**C**TG**T**C**C**G**A**AG **T**TC**C**TC**G**AT**T**GT**A**CT**G**CAA**A**TT**T**TCATGATCTCAGTGAAC-3′ were used to amplify PB1mut ORF. Forward primer 5′-CAGCTAGCATGGA**G**C**G**GA**T**C AA**G**GA**G**T**T**G**C**G**G**AA**C**TT**G**ATGTCGCAGTCTCGCAC-3′ and reverse primers 5′-TG**T**GA**A**TCCGT**C**AA**G**AT**A**G**AGCTA**T**C**T**C**T**CTT**T**C**T**CTTCAT**C** AC**T**A**GT**ACCACGTCTCCTTGCCC-3′ and 5′-GACTCGAGCTA**G**TT**A**AT**A** GCCAT**A**CG**G**ATCCT**C**TTA**G**T**T**GCCGTTTG**T**GA**A**TCCGT**C**AA**G**-3′ were used to amplify PB2mut ORF. Forward primer 5′-CAGCTAGCATGGA**G**GA **C**TTCGT**A**A**G**G**C**A**G**TG**T**TTT**A**ACCC**A**ATGAT**C**GT**T**GA**A**CT**C**G**C**A**G**A**G**A **A**G**A**C**G**ATGAA**G**GAGTATGGGGAGG-3′ and reverse primer 5′-GTCTCG AGCTA**T**G**A**T**A**G**C**GC**G**TG**C**GT**C**AA**A**AAAGAATT**A**AACCA**GCTG**GC**G**TT AAGCAAAACCCAG-3′ were used to amplify the PAmut ORF. The boldface letters in these primer sequences designate mutated nucleotides. Site-directed mutagenesis was used to remove one NheI site in the PB1mut ORF (A1143G) and one NheI site in the PAmut ORF (A1233G). The PB1mut, PB2mut, and PAmut ORFs were subsequently used to replace the green fluorescent protein (GFP) ORF of previously constructed plasmid pDZ-GFP-2 using the NheI and XhoI sites (6), generating the NA-PB1mut-NA, NA-PB2mut-NA, and NA-PAmut-NA constructs (Fig. 1A).

(ii) Generation of PB1-GFP-PB1, PB2-GFP-PB2, and PA-GFP-PA constructs. PB1-GFP-PB1, PB2-GFP-PB2, and PA-GFP-PA constructs were generated as shown in Fig. 1A (right). The 2.7-kb KpnI fragment from previously constructed pDZ-PB1 plasmid (25) was transferred to the KpnI site of the pUC18 vector and subjected to site-directed mutagenesis to mutate six ATGs (A25T, A29T, A71T, A119T, A142T, and A146T) and to generate one NheI site (A148G, G151A, and T152G) and one XhoI site (C2184T and A2185C). The 2.7-kb PB1 KpnI fragment was then transferred back to the pDZ vector (25) (in which the NheI and XhoI sites had been removed), resulting in plasmid pDZ-PB1-ps (ps designates packaging sequences). Following the same strategy, three ATGs (A28T, A58T, and A109T) were mutated in the PB2 gene, and four mutations (C153G, C155T, T2175C, and C2177A) were introduced to generate one NheI site and one XhoI site, resulting in plasmid pDZ-PB2-ps; six ATGs (A25T, A45T, A58T, A85T, A95T, and A138T) were mutated in the PA gene, and five mutations (A142T, C143A, T144G, T2052C, and A2055G) were introduced to generate one NheI site and one XhoI site, resulting plasmid pDZ-PA-ps. The GFP ORF was digested from the pDZ-GFP-2 plasmid (6) and ligated to the NheI and XhoI sites of plasmids pDZ-PB1-ps, pDZ-PB2-ps, and pDZ-PA-ps, respectively, generating the PB1-GFP-PB1, PB2-GFP-PB2, and PA-GFP-PA constructs (Fig. 1A).

(iii) Generation of PB1-HA(HK)-PB1, PB2-HA(HK)-PB2 constructs. The PB1-HA(HK)-PB1 and PB2-HA(HK)-PB2 constructs were generated as shown in Fig. 2A. The A/HK/1/68 HA ORF was amplified by PCR from the pCAGGS-HK HA plasmid (27) using forward primer 5′-CAGCTAGCATGAA GACCATCATTGCTTTGAGCTACATTTTC-3′ and reverse primer 5′-GTCT CGAGTCAAATGCAAATGTTGCACCTAATGTTGCCTCTC-3′. One internal XhoI site was deleted using site-directed mutagenesis. The full-length A/HK/1/68 HA ORF was then used to replace the GFP gene of the PB1-GFP-PB1 and PB2-GFP-PB2 constructs (Fig. 1A), generating the PB1-HA(HK)-PB1 and PB2-HA(HK)-PB2 constructs (Fig. 2A). The GFP gene of the PB1-GFP-PB1 construct (Fig. 1A) was also replaced by a *Renilla* luciferase ORF amplified from plasmid pRLtk (Promega), generating the PB1-Luc-PB1 construct, which was used to rescue the control virus, −PB1(ps)+Luc (Fig. 3A).

The sequences of the chimeric segments generated in this study are listed in the supplemental material.

Reverse genetics for recombinant viruses. The method for generating recombinant influenza viruses was performed as described previously (3, 6, 25).

Acrylamide gel electrophoresis of purified vRNA. The viruses were grown in 10-day-old eggs at 37°C and were subsequently processed by using a previously reported method (6). Briefly, virus was purified and RNA was isolated and run on a 2.8% denaturing polyacrylamide gel, which was then stained with a silver staining kit (Invitrogen).

Western blotting. To detect the viral protein within virions, viruses [rA/PR/8/34, X31, −PB1(ps)+HK HA, and −PB2(ps)+HK HA] were grown in embyonated chicken eggs at 37°C and concentrated through a 30% sucrose cushion. The pelleted virions were suspended in phosphate-buffered saline (PBS) and dissolved in 2× protein loading buffer (100 mM Tris-HCl [pH 6.8], 4% sodium dodecyl sulfate, 20% glycerol, 5% β-mercaptoethanol, 0.2% bromophenol blue). To detect the expression of viral proteins in infected cells, 80% confluent MDCK cell monolayers in six-well dishes were infected with viruses [rA/PR/8/34, X31, −PB1(ps)+HK HA, and −PB2(ps)+HK HA] at a multiplicity of infection (MOI) of 10 to 0.0001. One day after infection, the cells were washed with PBS and harvested and lysed in 2× protein loading buffer. The protein lysates were separated on a 10% sodium dodecyl sulfate–polyacrylamide gel and transferred onto a nitrocellulose membrane (Whatman, Inc.). The membrane was then probed with mouse monoclonal antibodies (MAbs) against A/PR/8/34 HA (PY102; 1:2,000 dilution) (26), A/PR/8/34 NP (HT103; 1:1,000 dilution) (21), A/HK/1/68 HA1 (66A6; 1:2,000 dilution) (27), and A/HK/1/68 HA2 (12D1; 1:2,000 dilution) (27).

Immunostaining of plaques. For plaque immunostaining, previous methods were followed (6, 14). A rabbit anti-A/PR/8/34 polyclonal antibody (1:2,000 dilution) was used for plaque visualization.

Viral growth kinetics. Ten-day-old embryonated chicken eggs were inoculated with influenza viruses (100 PFU/egg) and incubated at 37°C. At 24, 48, and 72 h postinoculation, the allantoic fluids were harvested and the titers of the viruses were determined by plaque assay or immunostaining of the plaques in MDCK cells. At each time point, three eggs were analyzed for each virus.

Mouse immunization and challenge. Eight-week-old female C57BL/6 mice (CRL) were anesthetized intraperitoneally with a mixture of ketamine and xylazine, and immunized intranasally with 50 μl of PBS or influenza viruses [−PB1(ps)+HK HA or −PB1(ps)+Luc, in a dose of 10^3 or 10^4 PFU/mouse]. The mice were monitored daily for weight loss over a 2-week period. Three weeks after immunization, mice were challenged by intranasal infection with either 100 50% mouse lethal doses (MLD_{50}) of A/PR/8/34 or 33.3 MLD_{50} of X31 virus. Again mice were monitored daily for weight loss or other signs of disease over a 2-week period. All procedures were performed in accordance with the guidelines of the Mount Sinai School of Medicine Institutional Animal Care and Use Committee.

Hemagglutination inhibition (HI) assay. Blood samples were collected from mice prior to vaccination (at day 0) and prior to challenge (at day 21). Receptor-destroying enzyme (Sigma) treatment was used to eliminate nonspecific inhibitors of hemagglutination. The protocols of the *WHO Manual on Animal Influenza Diagnosis and Surveillance* were followed (28a).

H1/H3 sandwich ELISA. For the sandwich enzyme-linked immunosorbent assay (ELISA), 96-well Immulon 2HB plates (Nunc) were coated with mouse anti-H3 HA MAb 66A6 (immunoglobulin G1 [IgG1]) (27) (5 μg/ml in PBS) by overnight incubation at 4°C. Plates were then blocked with 1% bovine serum albumin (BSA) in PBS at room temperature for 30 min. Two-fold dilutions of intact egg grown virus were added, and plates were incubated for 3 h at 37°C. The subtype H1 HA protein on captured virus particles was then probed with 1 μg/ml anti-H1 HA antibody C179 (mouse IgG2a) (20) for 3 h at 37°C and detected by goat anti-mouse IgG2a conjugated with alkaline phosphatase (AP) (Southern Biotech) (1:2,000 dilution).

RESULTS

Generation of recombinant A/PR/8/34 viruses carrying a ninth GFP segment. At restrictive temperature, a temperature-sensitive influenza A virus has been shown capable of containing two sets of nonstructural protein (NS) segment-specific packaging signals located in two different segments: one set was derived from an NS segment that has a temperature-sensitive defect in the NS1 gene, and a second set was from the segment that carries a wild-type NS1 gene (2). In the present

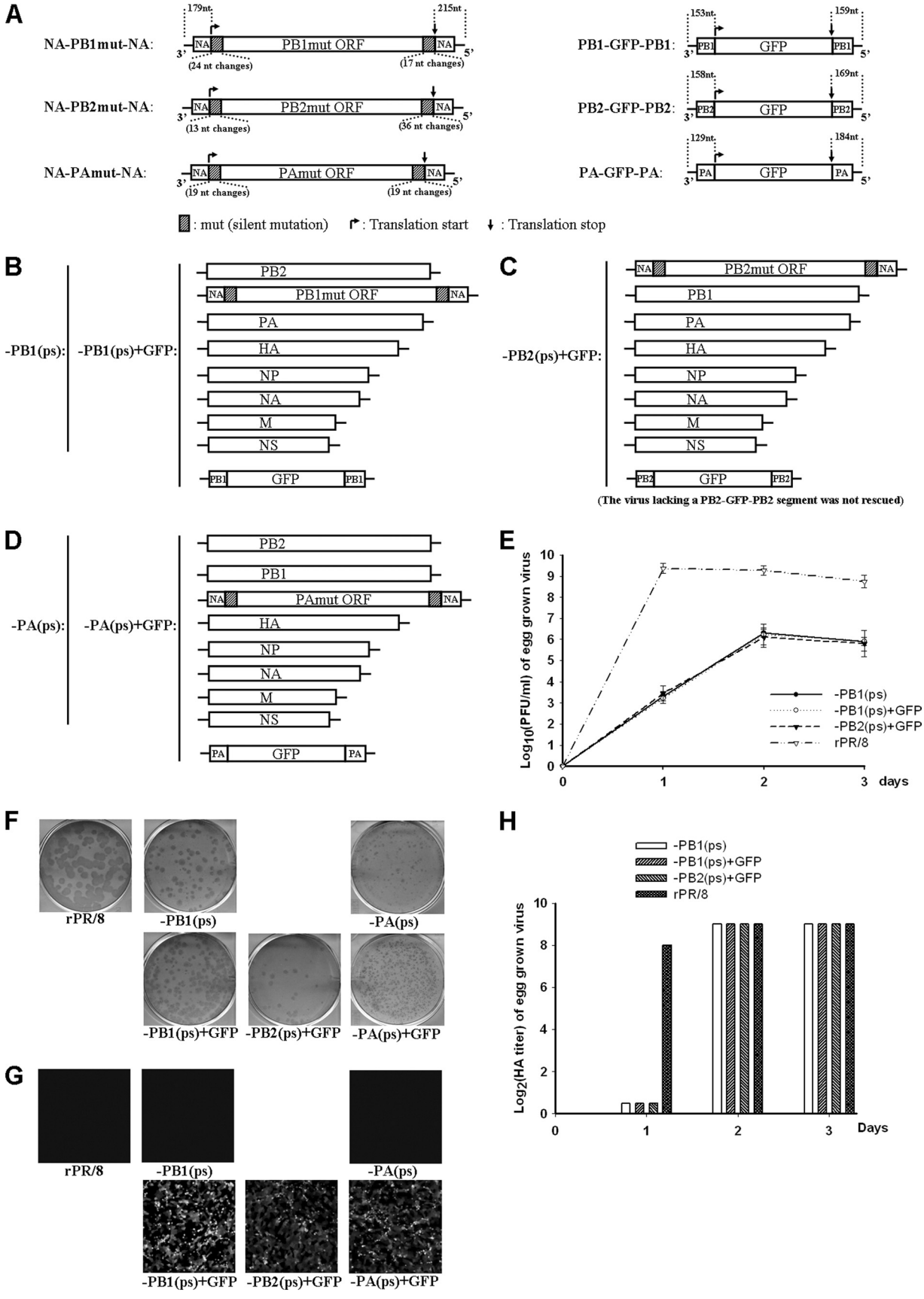
A
NA-PB1mut-NA:
179nt.
215nt.
NA
PB1mut ORF
NA
3'
5'
(24 nt changes)
(17 nt changes)
NA-PB2mut-NA:
NA
PB2mut ORF
NA
(13 nt changes)
(36 nt changes)
NA-PAmut-NA:
NA
PAmut ORF
NA
(19 nt changes)
(19 nt changes)
PB1-GFP-PB1:
153nt.
159nt.
PB1
GFP
PB1
PB2-GFP-PB2:
158nt.
169nt.
PB2
GFP
PB2
PA-GFP-PA:
129nt.
184nt.
PA
GFP
PA
: mut (silent mutation)
: Translation start
: Translation stop
B
-PB1(ps):
-PB1(ps)+GFP:
PB2
NA
PB1mut ORF
NA
PA
HA
NP
NA
M
NS
PB1
GFP
PB1
C
-PB2(ps)+GFP:
NA
PB2mut ORF
NA
PB1
PA
HA
NP
NA
M
NS
PB2
GFP
PB2
(The virus lacking a PB2-GFP-PB2 segment was not rescued)
D
-PA(ps):
-PA(ps)+GFP:
PB2
PB1
NA
PAmut ORF
NA
HA
NP
NA
M
NS
PA
GFP
PA
E
Log10(PFU/ml) of egg grown virus
10
9
8
7
6
5
4
3
2
1
0
0
1
2
3
days
-PB1(ps)
-PB1(ps)+GFP
-PB2(ps)+GFP
rPR/8
F
rPR/8
-PB1(ps)
-PA(ps)
-PB1(ps)+GFP
-PB2(ps)+GFP
-PA(ps)+GFP
G
rPR/8
-PB1(ps)
-PA(ps)
-PB1(ps)+GFP
-PB2(ps)+GFP
-PA(ps)+GFP
H
-PB1(ps)
-PB1(ps)+GFP
-PB2(ps)+GFP
rPR/8
Log2(HA titer) of egg grown virus
10
8
6
4
2
0
0
1
2
3
Days

study, to determine whether influenza A virus was able to incorporate two copies of NA segment-specific packaging sequences, the packaging signals of the PB1 segment were switched to those from the NA segment (Fig. 1A, left), while the original NA segment was unchanged. To accomplish this, the A/PR/8/34 PB1 ORF that carried serial synonymous mutations at the two ends, named PB1mut (Fig. 1A, left), was flanked by the NA segment-specific packaging sequences (including the 3′ and 5′ NCRs, as well as the terminal coding sequence of the NA ORF), thus generating the NA-PB1mut-NA segment (Fig. 1A, left). Based on our previous findings that the partial packaging signals in the HA or NS ORF region can affect viral RNA incorporation (7), we decided to silently mutate the two ends of the PB1 ORF. The synonymous mutations in the PB1mut ORF region include 24-nucleotide (nt) and 17-nt changes in the 3′- and 5′-proximal regions, respectively. The ATGs in the 3′-proximal NA region of the chimeric NA-PB1mut-NA segment were all mutated by site-directed mutagenesis so that translation would be initiated at the PB1mut gene start codon. Based on our previous findings for the HA and NS segments (7) and data from other studies (4, 8, 9, 11–13), we surmised that this chimeric NA-PB1mut-NA construct in Fig. 1A would most likely utilize the flanking NA packaging signals due to the absence of proper PB1-specific packaging sequences.

Using reverse genetics, a −PB1(ps) virus that carries seven wild-type A/PR/8/34 RNA segments (PB2, PA, HA, NP, NA, M, and NS) and one chimeric NA-PB1mut-NA segment was successfully rescued (Fig. 1B). The −PB1(ps) virus was attenuated compared with wild-type A/PR/8/34 virus, with lower titers in eggs and smaller plaques in MDCK cells (Fig. 1E and F). To determine whether the −PB1(ps) virus was able to incorporate a ninth segment that had PB1 segment-specific packaging signals, we generated a PB1-GFP-PB1 construct that carried 153 nt of PB1 packaging sequences in the 3′ end and 159 nt in the 5′ end (Fig. 1A, right). These 153-nt and 159-nt sequences consisted of both NCRs and terminal coding region packaging sequences and the six ATGs located in the 3′ 153-nt PB1 packaging sequences were all mutated by site-directed mutagenesis. We then successfully generated the −PB1(ps)+GFP virus that had all eight segments of the −PB1(ps) virus and a ninth GFP segment with PB1 segment-specific packaging signals (Fig. 1B). −PB1(ps)+GFP virus exhibited similar growth characteristics to the −PB1(ps) virus, with similar titers in eggs and similar plaque phenotypes in MDCK cells (Fig. 1E and F). The −PB1(ps)+GFP virus was stable, and GFP expression in infected cells (Fig. 1G) was maintained over 5 passages in eggs by the limiting dilution technique. The percentage of GFP-expressing plaques formed by the −PB1(ps)+GFP virus also did not change over 5 passages in eggs (see the supplemental material).

Following the same strategy, the packaging signals of the PB2 and PA segments were also each replaced with those of NA. Chimeric constructs NA-PB2mut-NA and NA-PAmut-NA were generated (Fig. 1A, left). The PB2mut ORF had 13-nt synonymous changes in the 3′ end and 36 nt in the 5′ end to inactivate the PB2 ORF region packaging signals, and the PAmut ORF region carried 19-nt synonymous changes in the 3′ end and the same number of changes in the 5′ end to inactivate the PA ORF region packaging signals (Fig. 1A, left). The two chimeric GFP constructs PB2-GFP-PB2 and PA-GFP-PA, which respectively carried PB2 and PA segment-specific packaging sequences, were made using the same method utilized to produce the PB1-GFP-PB1 construct (Fig. 1A, right). The 3 ATGs in the 3′-end 158-nt PB2 packaging sequences of the PB2-GFP-PB2 and 3 ATGs in the 3′-end 129-nt PA packaging sequences of the PA-GFP-PA construct were all mutated to TTGs in order for the GFP gene to utilize its own initiation codon (Fig. 1A, right). For the PB2 segment, we were unable to rescue a virus that has seven wild-type A/PR/8/34 RNA segments (PB1, PA, HA, NP, NA, M, and NS) and one chimeric segment, NA-PB2mut-NA. However, when a ninth PB2-GFP-PB2 construct was added, the −PB2(ps)+GFP virus was successfully rescued (Fig. 1C). The −PB2(ps)+GFP virus grew in eggs to a titer similar to that of the −PB1(ps)+GFP virus (Fig. 1E), but it produced slightly smaller plaques in MDCK cells (Fig. 1F). The expression of GFP in infected cells (Fig. 1G) and the percentage of GFP-expressing plaques (see the

FIG. 1. Generation of influenza viruses with a ninth GFP segment. (A) Generation of NA-PB1mut-NA, NA-PB2mut-NA, NA-PAmut-NA, PB1-GFP-PB1, PB2-GFP-PB2, and PA-GFP-PA constructs. To generate the NA-PB1mut-NA, NA-PB2mut-NA, and NA-PAmut-NA constructs, the PB1mut, PB2mut, or PAmut ORF regions were obtained by PCR, and serial silent mutations were introduced into the 3′- and 5′-proximal regions: 24 and 17 nt for PB1mut, 13 and 36 nt for PB2mut, and 19 and 19 nt for PAmut (Materials and Methods). The PB1mut, PB2mut, or PAmut ORFs were then flanked by 179 nt of NA packaging sequences in the 3′ end and 215 nt of NA packaging sequences in the 5′ end. The ATGs located on the 179 nt of NA packaging sequences were all mutated to TTGs. To generate the PB1-GFP-PB1, PB2-GFP-PB2, and PA-GFP-PA constructs, the GFP ORF region was flanked by the PB1, PB2, and PA packaging sequences, respectively. The PB1 packaging sequences included 153 nt of PB1 3′ end and 159 nt of PB1 5′ end, the PB2 packaging sequences included 158 nt of PB2 3′ end and 169 nt of PB2 5′ end, and the PA packaging sequences included 129 nt of PA 3′ end and 184 nt of PA 5′ end. The ATGs located on the 3′ ends of the PB1, PB2, and PA packaging sequences were all mutated to TTGs. The translation start and stop codons of each construct are indicated by arrows. (B) Genome structure of −PB1(ps) and −PB1(ps)+GFP viruses. Seven A/PR/8/34 ambisense plasmids (pDZ-PB2, pDZ-PA, pDZ-HA, pDZ-NP, pDZ-NA, pDZ-M, and pDZ-NS) and one chimeric construct (NA-PB1mut-NA) were used to generate the −PB1(ps) virus by reverse genetics (3, 25). For the rescue of −PB1(ps)+GFP virus, a ninth PB1-GFP-PB1 construct was included. (C) Genome structure of −PB2(ps)+GFP virus. Similar to the −PB1(ps)+GFP virus in panel B, the virus contained a chimeric NA-PB2mut-NA segment instead of a wild-type PB2, seven A/PR/8/34 segments (PB1, PA, HA, NP, NA, M, and NS), and a ninth PB2-GFP-PB2 chimeric segment. The virus lacking a ninth PB2-GFP-PB2 segment was not rescued. (D) Genome structure of −PA(ps) and −PA(ps)+GFP viruses. Similar to −PB1(ps) in panel B, the −PA(ps) virus contained a chimeric NA-PAmut-NA segment instead of a wild-type PA and seven A/PR/8/34 segments (PB2, PB1, HA, NP, NA, M, and NS). The −PA(ps)+GFP virus contained a ninth PA-GFP-PA chimeric segment. (E) Growth curves of viruses in 10-day-old embryonated chicken eggs at 37°C. The error bars represent standard deviations. (F) Immunostaining of the plaques formed in MDCK cells by the recombinant viruses 2 days postinfection. (G) GFP expression of recombinant viruses in 293T cells 1 day postinfection (MOI of 0.5). The viruses used for infection had been passaged five to 10 times in eggs. (H) Hemagglutination assay of viruses grown in 10-day-old embryonated chicken eggs at 37°C.

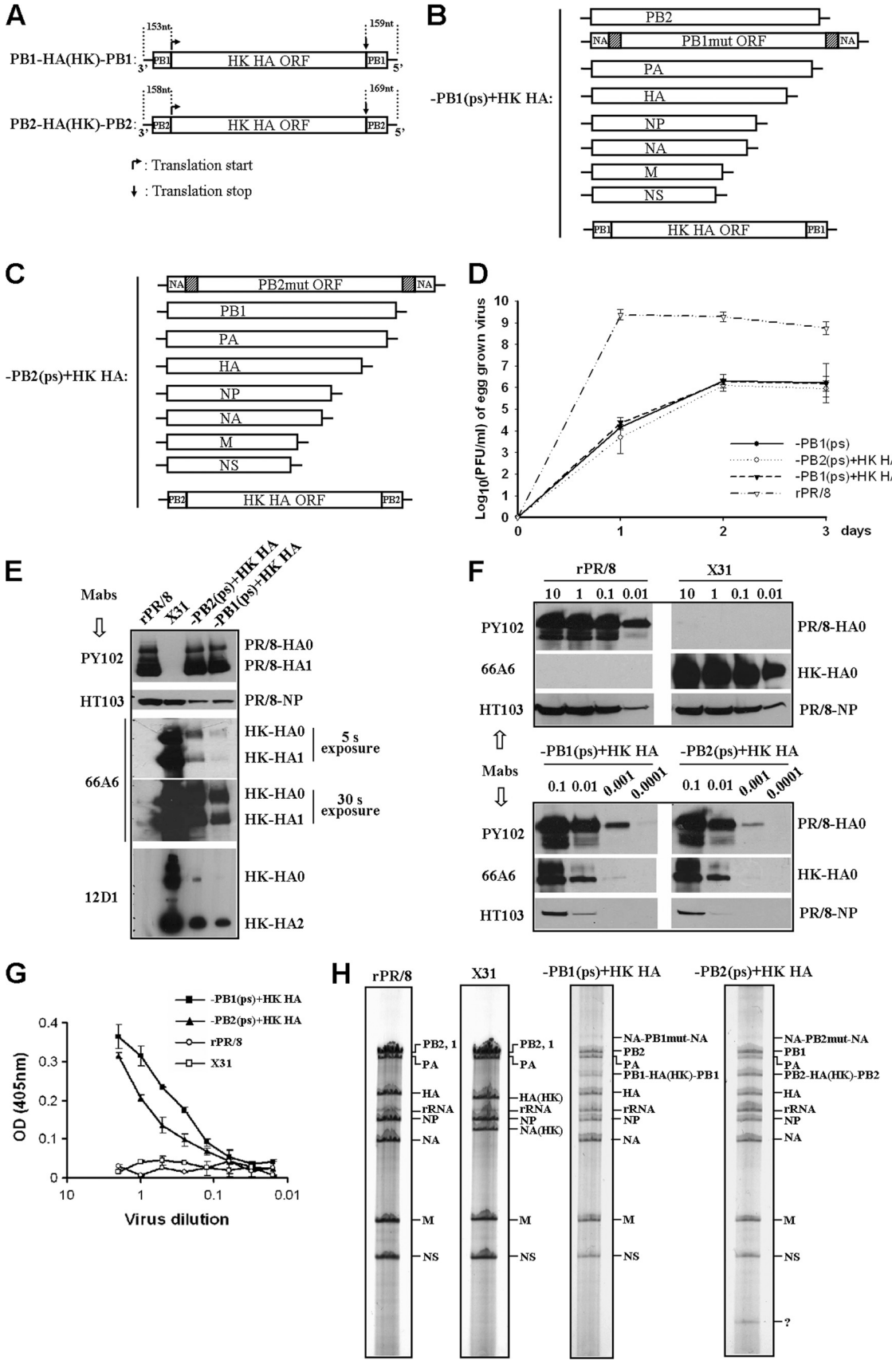
A
PB1-HA(HK)-PB1:
153nt
159nt
PB1
HK HA ORF
PB1
3'
5'
PB2-HA(HK)-PB2:
158nt
169nt
PB2
HK HA ORF
PB2
: Translation start
: Translation stop
B
-PB1(ps)+HK HA:
PB2
NA
PB1mut ORF
NA
PA
HA
NP
NA
M
NS
PB1
HK HA ORF
PB1
C
-PB2(ps)+HK HA:
NA
PB2mut ORF
NA
PB1
PA
HA
NP
NA
M
NS
PB2
HK HA ORF
PB2
D
Log10(PFU/ml) of egg grown virus
days
-PB1(ps)
-PB2(ps)+HK HA
-PB1(ps)+HK HA
rPR/8
E
Mabs
rPR/8
X31
-PB2(ps)+HK HA
-PB1(ps)+HK HA
PY102
PR/8-HA0
PR/8-HA1
HT103
PR/8-NP
66A6
HK-HA0
HK-HA1
5 s exposure
HK-HA0
HK-HA1
30 s exposure
12D1
HK-HA0
HK-HA2
F
rPR/8
X31
10 1 0.1 0.01
10 1 0.1 0.01
PY102
PR/8-HA0
66A6
HK-HA0
HT103
PR/8-NP
-PB1(ps)+HK HA
-PB2(ps)+HK HA
Mabs
0.1 0.01 0.001 0.0001
0.1 0.01 0.001 0.0001
PY102
PR/8-HA0
66A6
HK-HA0
HT103
PR/8-NP
G
-PB1(ps)+HK HA
-PB2(ps)+HK HA
rPR/8
X31
OD (405nm)
Virus dilution
H
rPR/8
X31
-PB1(ps)+HK HA
-PB2(ps)+HK HA
PB2, 1
PA
HA
rRNA
NP
NA
M
NS
PB2, 1
PA
HA(HK)
rRNA
NP
NA(HK)
M
NS
NA-PB1mut-NA
PB2
PA
PB1-HA(HK)-PB1
HA
rRNA
NP
NA
M
NS
NA-PB2mut-NA
PB1
PA
PB2-HA(HK)-PB2
HA
rRNA
NP
NA
M
NS
?

supplemental material) were also stably maintained over at least five passages in embryonated chicken eggs by the limiting dilution technique. For the PA segment, we successfully rescued a −PA(ps) virus that has seven wild-type A/PR/8/34 segments (PB2, PB1, HA, NP, NA, M, and NS) and one chimeric segment, NA-PAmut-NA (Fig. 1D). The −PA(ps)+GFP virus carrying the ninth PA-GFP-PA segment was also successfully rescued (Fig. 1D). The −PA(ps) and −PA(ps)+GFP viruses were more attenuated than the −PB1(ps), −PB1(ps)+GFP, and −PB2(ps)+GFP viruses, growing to lower titers in eggs (data not shown) and generating smaller plaques in MDCK cells (Fig. 1F). Due to small plaque size, the infectious titers of the −PA(ps) and −PA(ps)+GFP viruses could not be accurately measured and we therefore did not further characterize their growth rates in eggs. The GFP expression by the −PA(ps)+GFP virus in infected cells (Fig. 1G) was, however, stably maintained over at least five passages in embryonated chicken eggs. Finally, although the infectious titers of the −PB1(ps), −PB1(ps)+GFP, and the −PB2(ps)+GFP viruses from eggs were much lower than that of recombinant A/PR/8/34 (rA/PR/8/34) virus (Fig. 1E), their hemagglutination assay titers were comparable to that of the rA/PR/8/34 virus 2 and 3 days postinoculation (Fig. 1H), suggesting that these viruses produced more defective virions than does the wild-type virus.

It should be noted that the number of synonymous mutations introduced to disrupt the packaging signals in the ORF region and the length of the flanking packaging sequences used in the chimeric constructs (Fig. 1A) were decided upon previous characterization of the A/WSN/33 viral RNA packaging signals (5, 10, 11, 13, 15).

In conclusion, we generated a novel approach to construct several nine-segment influenza viruses simply by manipulating the RNA packaging sequences. The resulting viruses were genetically stable and carried an extra GFP segment. Linearity between dilutions and plaque numbers was also observed for these nine-segment viruses, suggesting indeed more than eight RNAs can be incorporated into one particle (data not shown).

Generation of recombinant influenza viruses carrying both A/PR/8/34(H1N1) and A/HK/1/68(H3N2) HAs. We next sought to determine whether our method for generating the nine-segment GFP-expressing virus could be used to generate influenza viruses coding for two subtypes of HA: the A/PR/8/34(H1N1) HA and the HA from A/HK/1/68(H3N2). To do this, the GFP ORF regions of the PB1-GFP-PB1 and PB2-GFP-PB2 constructs (Fig. 1A, right) were each replaced by the A/HK/1/68 HA ORF, generating the PB1-HA(HK)-PB1 and PB2-HA(HK)-PB2 constructs (Fig. 2A). Using reverse genetics, we were able to successfully rescue two nine-segment viruses named −PB1(ps)+HK HA (Fig. 2B) and −PB2(ps)+HK HA (Fig. 2C). The −PB1(ps)+HK HA virus and the −PB2(ps)+HK HA virus had similar growth characteristics to the −PB1(ps)+GFP and −PB2(ps)+GFP viruses (Fig. 1E and 2D), respectively. In order to show that both the A/PR/8/34 and the A/HK/1/68 HAs were incorporated into particles of the −PB1(ps)+HK HA and −PB2(ps)+HK HA viruses, four viruses (rA/PR/8/34; X31, which has six A/PR/8/34 internal genes and the A/HK/1/68 HA and NA genes; −PB2(ps)+HK HA; and −PB1(ps)+HK HA) were grown in eggs and concentrated by passing through a sucrose cushion. Western blotting was then performed to detect the A/PR/8/34 and A/HK/1/68 HAs in purified virions (Fig. 2E). The results showed that when the same amounts of virus proteins were loaded, the −PB1(ps)+HK HA and −PB2(ps)+HK HA viruses had similar levels of A/PR/8/34 HA protein compared with the wild-type rA/PR/8/34 virus; this includes uncleaved HA0 and cleaved HA1 detected by the mouse MAb PY102 (Fig. 2E). Also, when comparable amounts of virus proteins were loaded, rA/PR/8/34 and X31 had the same amount of NP protein detected by MAb HT103 (Fig. 2E). However, for the −PB1(ps)+HK HA and −PB2(ps)+HK HA chimeric viruses, the NP levels were about five times lower than those of rA/PR/8/34 and X31 viruses (Fig. 2E), indicating a less-efficient RNP incorporation by the nine-segment viruses. Both HA0 and HA1 from A/HK/1/68 were detected in the −PB1(ps)+HK HA and the −PB2(ps)+HK HA virus parti-

FIG. 2. Generation of nine-segment influenza viruses carrying both subtype H1 and H3 HAs. (A) Generation of PB1-HA(HK)-PB1 and PB2-HA(HK)-PB2 constructs. The A/HK/1/68 HA ORF was amplified from a pCAGGS-HK HA plasmid (27) by PCR and used to replace the GFP ORF of PB1-GFP-PB1 and PB2-GFP-PB2 constructs in Fig. 1A, generating the PB1-HA(HK)-PB1 and PB2-HA(HK)-PB2 constructs. (B) Genome structure of −PB1(ps)+HK HA virus. Similar to −PB1(ps)+GFP virus in Fig. 1B, the virus contained a chimeric NA-PB1mut-NA segment instead of a wild-type PB1, seven A/PR/8/34 segments (PB2, PA, HA, NP, NA, M, and NS), and a ninth PB1-HA(HK)-PB1 chimeric segment. (C) Genome structure of −PB2(ps)+HK HA virus. The chimeric PB2-HA(HK)-PB2 segment was used to replace the PB2-GFP-PB2 of the −PB2(ps)+GFP virus in Fig. 1C, generating the −PB2(ps)+HK HA virus. (D) Growth curves of viruses in 10-day-old embryonated chicken eggs at 37°C. The error bars represent standard deviations. (E) Western blot to detect the A/PR/8/34 and A/HK/1/68 HAs in purified virions. Viruses [rA/PR/8/34, X31, −PB2(ps)+HK HA and −PB1(ps)+HK HA] were grown in eggs at 37°C and purified through a 30% sucrose cushion. A Western blot was performed to detect the presence of NP and HA proteins using specific mouse monoclonal antibodies: PY102 for A/PR/8/34 HA0 and HA1 (26), HT103 for A/PR/8/34 NP (21), 66A6 for A/HK/1/68 HA0 and HA1, and 12D1 for A/HK/1/68 HA0 and HA2 (27). (F) Western blot to detect the A/PR/8/34 and A/HK/1/68 HAs in virus-infected MDCK cells. MDCK monolayers were infected by viruses [rA/PR/8/34, X31, −PB1(ps)+HK HA, and −PB2(ps)+HK HA] at an MOI of 10 to 0.0001. One day postinfection, the cells were washed with PBS and harvested using 2× protein loading buffer (100 mM Tris-HCl [pH 6.8], 4% sodium dodecyl sulfate, 20% glycerol, 5% β-mercaptoethanol, 0.2% bromophenol blue) and run on a 10% SDS-polyacrylamide gel electrophoresis (PAGE) gel. The A/PR/8/34 HA0, NP, and A/HK/1/68 HA0 were detected by monoclonal antibodies PY102, HT103, and 66A6, respectively (21, 26, 27). (G) H1/H3 sandwich ELISA to determine whether both subtype H1 and H3 HA proteins were incorporated into the same particles of the −PB1(ps)+HK HA and −PB2(ps)+HK HA viruses (see Materials and Methods). OD, optical density. The error bars represent standard deviations. (H) Analysis of the vRNA genome packaging efficiency of the recombinant viruses. Four recombinant viruses [rA/PR/8/34, X31, −PB1(ps)+HK HA, and −PB2(ps)+HK HA] were grown in eggs at 37°C, and purified viral RNA was separated (0.5 μg/lane) on a 2.8% acrylamide gel and visualized by silver staining. The rRNA band was confirmed based on size and previously reported findings. The identity of an additional band marked with "?" is unknown.

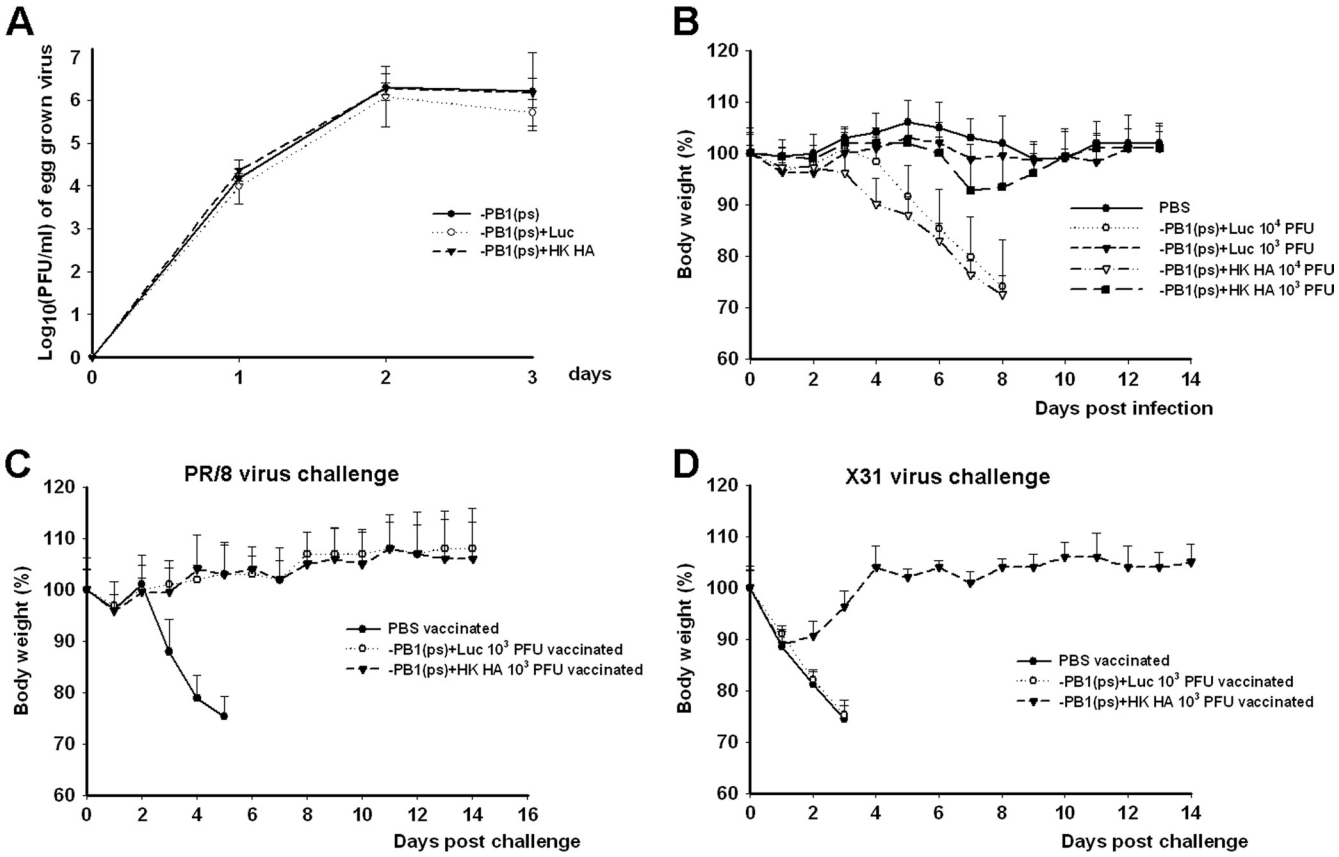

FIG. 3. Immunization of mice with −PB1(ps)+HK HA virus conferred complete protection from lethal challenges of rA/PR/8/34 and X31 viruses. (A) Growth curves of viruses in 10-day-old embryonated chicken eggs at 37°C. (B) Pathogenicity of −PB1(ps)+HK HA and −PB1(ps)+Luc viruses. Groups of C57BL/6 mice were given PBS, −PB1(ps)+HK HA virus, or the −PB1(ps)+Luc virus, at 10^3 or 10^4 PFU through the intranasal route, and observed for 2 weeks for weight loss and signs of disease. The average body weights of animals in each group are indicated as percentages of the original body weights. (C) rA/PR/8/34 virus challenge experiment. Three weeks after the infection, the groups of mice that received PBS, 10^3 PFU −PB1(ps)+HK HA virus, and 10^3 PFU −PB1(ps)+Luc virus were challenged intranasally with 100 MLD_{50} of rA/PR/8/34 virus. The mice were then observed daily for 2 weeks for body weight loss and signs of disease. (D) X31 virus challenge experiment. X31 virus challenge was performed as in panel C, except that the groups of mice were challenged by using 33 MLD_{50} of X31 virus instead of rA/PR/8/34 virus. The error bars in panels A to D represent standard deviations.

cles using MAb 66A6; notably, when normalized for total protein, H3 HA incorporation by the chimeric viruses was much lower than incorporation by the X31 virus, with the lowest levels seen in the −PB1(ps)+HK HA virus (Fig. 2E). The Western blot using MAb 12D1 to detect A/HK/1/68 HA0 and cleaved HA2 showed similar results (Fig. 2E). We then used Western blotting to detect the expression of both A/PR/8/34 and A/HK/1/68 HAs by the −PB1(ps)+HK HA and −PB2(ps)+HK HA viruses in infected cells (Fig. 2F). As expected, both A/PR/8/34 and A/HK/1/68 HAs were detected in MDCK cells infected by these viruses (Fig. 2F, lower panel). In contrast, as with Fig. 2E, cells infected with rA/PR/8/34 virus expressed only A/PR/8/34 HA and the X31 virus-infected cells expressed only H3 HA (Fig. 2F, upper panel).

Finally, a sandwich ELISA was performed to confirm that both subtype H1 and H3 HA proteins were incorporated into the nine-segment virus particles (Fig. 2G). Ninety-six-well plates were coated with MAb 66A6 (27) to capture intact virus particles in an H3-dependent manner. Virus particles were then probed for H1 content with MAb C179, an antibody with activity against subtype H1 and H2 HA but which does not react with H3 HA (20). Signals were detected for the two nine-segment viruses, indicating that indeed two types of HA proteins were incorporated into the virus particles. In contrast, both rA/PR/8/34 and X31 viruses gave negative results (Fig. 2G).

In conclusion, we successfully rescued two recombinant viruses, each of which carried two subtypes of HA: one A/PR/8/34(H1N1) HA and one A/HK/1/68(H3N2) HA. Both HAs were incorporated into virus particles and were expressed in virus-infected MDCK cells.

To determine the RNA packaging efficiencies of the recombinant −PB1(ps)+HK HA and −PB2(ps)+HK HA viruses, RNA was isolated from the purified viruses and resolved on a 2.8% acrylamide gel followed by silver staining (Fig. 2H). The X31 virus has six A/PR/8/34 internal genes along with the A/HK/1/68 HA and NA segments which migrated to distinct positions from those of the A/PR/8/34 HA and NA (Fig. 2H). By comparing densities of bands, we observed that the −PB1(ps)+HK HA virus inefficiently incorporated the NA-PB1mut-NA segment. The PB1-HA(HK)-PB1 segment was also packaged somewhat inefficiently when compared with the

TABLE 1. Hemagglutination inhibitory activity against rA/PR/8/34 and X31 viruses of sera from mice immunized with nine-segment viruses

Vaccine	Mouse	Titer against:			
		rA/PR/8/34		X31	
		Preimmune	Postvaccination	Preimmune	Postvaccination
PBS	1	<10	<10	<10	<10
	2	<10	<10	<10	<10
	3	<10	<10	<10	<10
	4	<10	<10	<10	<10
	5	<10	<10	<10	<10
−PB1(ps)+Luc	1	<10	160	<10	<10
	2	<10	320	<10	<10
	3	<10	160	<10	<10
	4	<10	320	<10	<10
	5	<10	320	<10	<10
−PB1(ps)+HK HA	1	<10	320	<10	20
	2	<10	640	<10	<10
	3	<10	320	<10	40
	4	<10	320	<10	20
	5	<10	320	<10	40

A/PR/8/34 HA segment (Fig. 2H). For the −PB2(ps)+HK HA virus, the NA-PB2mut-NA segment was inefficiently packaged. In contrast, the PB2-HA(HK)-PB2 segment was packaged efficiently, at a level similar to that of A/PR/8/34 HA (Fig. 2H).

Immunization of mice with a recombinant nine-segment virus with two HAs conferred protection from lethal challenges of rA/PR/8/34 and X31 viruses. To test whether the nine-segment influenza viruses carrying two subtypes of HA could be used as live vaccines, mouse challenge experiments were conducted. The −PB1(ps)+HK HA virus was arbitrarily chosen for the study. As a negative control immunogen, we used the −PB1(ps)+Luc virus, which carries a ninth PB1-Luc-PB1 instead of a PB1-HA(HK)-PB1 segment (Fig. 2B; see the supplemental material and Materials and Methods). Both −PB1(ps)+Luc and −PB1(ps)+HK HA viruses grew to similar titers as the −PB1(ps) virus in eggs (Fig. 3A). To test whether the nine-segment viruses were pathogenic in mice, groups of 8-week-old female C57BL/6 mice were given PBS, −PB1(ps)+HK HA virus, or −PB1(ps)+Luc virus, at either 10^3 or 10^4 PFU by intranasal administration (Fig. 3B). The mice infected with 10^4 PFU of either −PB1(ps)+Luc or −PB1(ps)+HK HA virus died or lost more than 25% of their initial body weight by day 8 postinfection (Fig. 3B). The group of mice given 10^3 PFU of −PB1(ps)+Luc exhibited little or no weight loss and exhibited no signs of disease, similar to the PBS group (Fig. 3B). The group of mice given 10^3 PFU of −PB1(ps)+HK HA virus lost approximately 5% of their body weight by day 7 postinfection followed by full recovery within 3 days; no other signs of disease were observed (Fig. 3B). Since administration of 10^3 PFU of either chimeric virus caused very little or no changes associated with illness, we considered exposure to this dose to be analogous with vaccination.

Three weeks postinfection, lethal virus challenge experiments were performed on the groups of mice infected with 10^3 PFU of −PB1(ps)+Luc virus, 10^3 PFU of −PB1(ps)+HK HA virus, or mice that were mock vaccinated with PBS. Mice were given 3,000 PFU (100 MLD_{50}) of rA/PR/8/34 virus by intranasal administration (Fig. 3C). In contrast to the PBS group, the groups vaccinated with either the −PB1(ps)+Luc or the −PB1(ps)+HK HA viruses were completely protected from lethal challenge: no loss of body weight or signs of disease were observed (Fig. 3C). Following the same methods, 10^7 PFU (33 MLD_{50}) of X31 virus was administered intranasally to a second set of mice that were mock vaccinated (PBS group), vaccinated with 10^3 PFU −PB1(ps)+Luc, or vaccinated with 10^3 PFU −PB1(ps)+HK HA virus (Fig. 3D). The groups of mice that were mock or −PB1(ps)+Luc vaccinated quickly lost 25% of their body weight in 3 days and were sacrificed. Although previous findings showed that cellular responses to the internal NP and M proteins conferred some protection against heterologous challenges (30), no protection was observed in the −PB1(ps)+Luc-vaccinated group, possibly due to the high dosage of challenge virus used. In contrast, vaccination with 10^3 PFU of −PB1(ps)+HK HA virus protected the mice from the lethal challenge with X31 virus. Average body weight was reduced by 10% on the day following challenge, and all mice quickly recovered (Fig. 3D).

Analysis of serum samples from this experiment indicated that by day 21 postvaccination, all animals vaccinated with 10^3 PFU of −PB1(ps)+HK HA virus produced hemagglutination-inhibiting antibodies against rA/PR/8/34 virus, with titers ranging from 320 to 640. Four out of five animals produced a low but detectable level of hemagglutination-inhibiting antibodies against X31 virus, with titers ranging from 20 to 40 (Table 1). As expected, animals vaccinated with 10^3 PFU of −PB1(ps)+Luc virus had only hemagglutination-inhibiting antibodies against rA/PR/8/34 virus, with titers ranging from 160 to 320 (Table 1). No hemagglutination-inhibiting antibodies against either rA/PR/8/34 or X31 virus were detected in serum from animals mock vaccinated with PBS.

In conclusion, we have shown that vaccination with 10^3 PFU of −PB1(ps)+HK HA virus was protective in mice against lethal challenge with influenza viruses from two separate subtypes: one H1N1 subtype (rA/PR/8/34) and one H3N2 subtype (X31).

DISCUSSION

In this study, we successfully generated two recombinant viruses named −PB1(ps) (Fig. 1B) and −PA(ps) (Fig. 1D), which lacked either PB1 or PA packaging sequences, respectively, and carried NA packaging sequences in their place. These viruses were viable; however, both the PB1 and the PA packaging signals were important for virus growth since the replacement of the PB1 segment by NA-PB1mut-NA or the PA segment by NA-PAmut-NA did have a significant effect on the packaging of both chimeric segments (Fig. 2H) as well as on virus growth rates (Fig. 1E and F). The ability to rescue both viruses might indicate that influenza virus genomic RNA packaging does not absolutely require PB1 or PA packaging signals. Based on our previous study of packaging of the HA and NS segments (7), we hypothesized that the two chimeric segments, NA-PB1mut-NA and NA-PAmut-NA (Fig. 1A, left), would likely utilize the flanking NA packaging signals instead of the PB1 and PA packaging signals, respectively. However, we could not rule out the possibility that the PB1 or PA ORF region carrying the serial synonymous mutations (Fig. 1A) partially retained the PB1 or PA packaging signals. Although 24- and 17-nt changes were introduced to the PB1 ORF and two sets of 19-nt changes were made in the PA ORF (Fig. 1A, left), some residual PB1 or PA packaging signals could still exist, enabling PB1 or PA segment-specific recognition (Fig. 1A, left). In this study, we were unable to rule out this possibility. Interestingly, both viruses were able to incorporate a ninth segment coding for GFP. When supplied with a ninth PB1-GFP-PB1 segment (Fig. 1A, right) flanked by the PB1 packaging sequence, the −PB1(ps) virus was able to stably incorporate it into the virus genome, generating the −PB1(ps)+GFP virus (Fig. 1B); likewise, the −PA(ps)+GFP virus was able to maintain an extra PA-GFP-PA segment flanked by the PA packaging signals (Fig. 1D). The generation of both viruses with an extra GFP segment reflected the tendency of influenza virus to have a complete set of packaging signals on its genomic RNAs.

For the PB2 segment, when the wild-type PB2 was replaced by the NA-PB2mut-NA chimeric segment (Fig. 1A, left), we were unable to rescue the virus. This was also seen in previous studies using A/WSN/33 virus in which mutation or deletion of the PB2 packaging sequences resulted in a more severe packaging defect than did manipulation of other segments (11, 15). However, when a ninth PB2-GFP-PB2 segment that carried PB2 packaging signals was included (Fig. 1A, right), the −PB2(ps)+GFP virus was successfully rescued (Fig. 1C). This result also reflected the preference of influenza virus to carry sets of eight unique packaging signals.

Using the strategy we designed for generation of the −PB1(ps)+GFP (Fig. 1B) and −PB2(ps)+GFP (Fig. 1C) viruses, we successfully rescued two recombinant viruses that encoded two different full-length HAs: both −PB1(ps)+HK HA virus (Fig. 2B) and −PB2(ps)+HK HA virus (Fig. 2C) encoded an A/PR/8/34 HA and an A/HK/1/68 HA. Thus, our study shows a novel approach to engineer viruses encoding two different HAs. These viruses are significantly attenuated compared to the wild-type virus, with lower growth rates in eggs and smaller plaques in MDCK cells (Fig. 1 and 2). The MLD_{50} of −PB1(ps)+HK HA was between 10^3 and 10^4 PFU (Fig. 3B), significantly higher than that of wild-type A/PR/8/34 virus, which has an MLD_{50} of about 30 PFU. Immunization of mice with 1,000 PFU of −PB1(ps)+HK HA virus completely protected them from the lethal challenge with rA/PR/8/34 virus or X31 virus, suggesting that this nine-segment virus strategy might be utilized for the development of bivalent live attenuated influenza vaccines. Although the −PB1(ps)+HK HA virus is potentially lethal to mice, a similar approach can be applied to other less virulent viruses for a live vaccine purpose. Current seasonal influenza vaccines must include three distinct influenza viruses: one A (H3N2) virus, one regular seasonal A (H1N1) virus, and one B virus. The bivalent, nine-segment influenza viruses described herein offer a means of combining two major antigens (e.g., H1 and H3 HAs) into one vaccine strain. This may be particular useful if the number of cocirculating influenza virus lineages increases to more than three: for example, in 2009, a novel swine origin influenza A virus of the H1N1 subtype, which is different from seasonal H1N1 virus, emerged from North America and caused an influenza pandemic. Furthermore, by carrying specific antigens on its ninth chimeric segment, this nine-segment influenza virus platform could also be applied to generate vaccines against other bacterial or viral pathogens.

ACKNOWLEDGMENTS

We thank John Steel and Gene S. Tan for helpful comments on the experiments.

This work was partially supported by NIH grants UO1 AI070469 (Live Attenuated Vaccines for Epidemic and Pandemic Flu), HHSN26620007000010C (Center for Research on Influenza Pathogenesis), 1RC1 AI086061-01 (Development of a Universal Influenza Virus Vaccine), and U54 AI057158-04 (Northeast Biodefense Center). Anice C. Lowen is a Parker B. Francis fellow in pulmonary research. Taia T. Wang was supported by NIH training grant T32 AI007647 and Mount Sinai Medical Scientists training grant T32 GM007280.

REFERENCES

1. **Duhaut, S. D., and J. W. McCauley.** 1996. Defective RNAs inhibit the assembly of influenza virus genome segments in a segment-specific manner. Virology **216:**326–337.
2. **Enami, M., G. Sharma, C. Benham, and P. Palese.** 1991. An influenza virus containing nine different RNA segments. Virology **185:**291–298.
3. **Fodor, E., L. Devenish, O. G. Engelhardt, P. Palese, G. G. Brownlee, and A. Garcia-Sastre.** 1999. Rescue of influenza A virus from recombinant DNA. J. Virol. **73:**9679–9682.
4. **Fujii, K., Y. Fujii, T. Noda, Y. Muramoto, T. Watanabe, A. Takada, H. Goto, T. Horimoto, and Y. Kawaoka.** 2005. Importance of both the coding and the segment-specific noncoding regions of the influenza A virus NS segment for its efficient incorporation into virions. J. Virol. **79:**3766–3774.
5. **Fujii, Y., H. Goto, T. Watanabe, T. Yoshida, and Y. Kawaoka.** 2003. Selective incorporation of influenza virus RNA segments into virions. Proc. Natl. Acad. Sci. U. S. A. **100:**2002–2007.
6. **Gao, Q., E. W. Brydon, and P. Palese.** 2008. A seven-segmented influenza A virus expressing the influenza C virus glycoprotein HEF. J. Virol. **82:**6419–6426.
7. **Gao, Q., and P. Palese.** 2009. Rewiring the RNAs of influenza virus to prevent reassortment. Proc. Natl. Acad. Sci. U. S. A. **106:**15891–15896.
8. **Gog, J. R., S. Afonso Edos, R. M. Dalton, I. Leclercq, L. Tiley, D. Elton, J. C. von Kirchbach, N. Naffakh, N. Escriou, and P. Digard.** 2007. Codon conservation in the influenza A virus genome defines RNA packaging signals. Nucleic Acids Res. **35:**1897–1907.
9. **Hutchinson, E. C., M. D. Curran, E. K. Read, J. R. Gog, and P. Digard.** 2008. Mutational analysis of cis-acting RNA signals in segment 7 of influenza A virus. J. Virol. **82:**11869–11879.
10. **Liang, Y., Y. Hong, and T. G. Parslow.** 2005. *cis*-Acting packaging signals in the influenza virus PB1, PB2, and PA genomic RNA segments. J. Virol. **79:**10348–10355.
11. **Liang, Y., T. Huang, H. Ly, T. G. Parslow, and Y. Liang.** 2008. Mutational analyses of packaging signals in influenza virus PA, PB1, and PB2 genomic RNA segments. J. Virol. **82:**229–236.
12. **Marsh, G. A., R. Hatami, and P. Palese.** 2007. Specific residues of the influenza A virus hemagglutinin viral RNA are important for efficient packaging into budding virions. J. Virol. **81:**9727–9736.
13. **Marsh, G. A., R. Rabadan, A. J. Levine, and P. Palese.** 2008. Highly con-

served regions of influenza a virus polymerase gene segments are critical for efficient viral RNA packaging. J. Virol. **82:**2295–2304.
14. **Matrosovich, M., T. Matrosovich, W. Garten, and H. D. Klenk.** 2006. New low-viscosity overlay medium for viral plaque assays. Virol. J. **3:**63.
15. **Muramoto, Y., A. Takada, K. Fujii, T. Noda, K. Iwatsuki-Horimoto, S. Watanabe, T. Horimoto, H. Kida, and Y. Kawaoka.** 2006. Hierarchy among viral RNA (vRNA) segments in their role in vRNA incorporation into influenza A virions. J. Virol. **80:**2318–2325.
16. **Nakajima, K., M. Ueda, and A. Sugiura.** 1979. Origin of small RNA in von Magnus particles of influenza virus. J. Virol. **29:**1142–1148.
17. **Nayak, D. P., N. Sivasubramanian, A. R. Davis, R. Cortini, and J. Sung.** 1982. Complete sequence analyses show that two defective interfering influenza viral RNAs contain a single internal deletion of a polymerase gene. Proc. Natl. Acad. Sci. U. S. A. **79:**2216–2220.
18. **Ng, S. S., O. T. Li, T. K. Cheung, J. S. Malik Peiris, and L. L. Poon.** 2008. Heterologous influenza vRNA segments with identical non-coding sequences stimulate viral RNA replication in trans. Virol. J. **5:**2.
19. **Noda, T., H. Sagara, A. Yen, A. Takada, H. Kida, R. H. Cheng, and Y. Kawaoka.** 2006. Architecture of ribonucleoprotein complexes in influenza A virus particles. Nature **439:**490–492.
20. **Okuno, Y., Y. Isegawa, F. Sasao, and S. Ueda.** 1993. A common neutralizing epitope conserved between the hemagglutinins of influenza A virus H1 and H2 strains. J. Virol. **67:**2552–2558.
21. **O'Neill, R. E., J. Talon, and P. Palese.** 1998. The influenza virus NEP (NS2 protein) mediates the nuclear export of viral ribonucleoproteins. EMBO J. **17:**288–296.
22. **Ozawa, M., K. Fujii, Y. Muramoto, S. Yamada, S. Yamayoshi, A. Takada, H. Goto, T. Horimoto, and Y. Kawaoka.** 2007. Contributions of two nuclear localization signals of influenza A virus nucleoprotein to viral replication. J. Virol. **81:**30–41.
23. **Ozawa, M., J. Maeda, K. Iwatsuki-Horimoto, S. Watanabe, H. Goto, T. Horimoto, and Y. Kawaoka.** 2009. Nucleotide sequence requirements at the 5′ end of the influenza A virus M RNA segment for efficient virus replication. J. Virol. **83:**3384–3388.
24. **Palese, P., and M. L. Shaw.** 2007. Orthomyxoviridae: the viruses and their replication, p. 1647–1689. *In* D. M. Knipe and P. M. Howley (ed.), Fields virology. Lippincott Williams & Wilkins, Philadelphia, PA.
25. **Quinlivan, M., D. Zamarin, A. Garcia-Sastre, A. Cullinane, T. Chambers, and P. Palese.** 2005. Attenuation of equine influenza viruses through truncations of the NS1 protein. J. Virol. **79:**8431–8439.
26. **Reale, M. A., A. J. Manheimer, T. M. Moran, G. Norton, C. A. Bona, and J. L. Schulman.** 1986. Characterization of monoclonal antibodies specific for sequential influenza A/PR/8/34 virus variants. J. Immunol. **137:**1352–1358.
27. **Wang, T. T., G. S. Tan, R. Hai, N. Pica, E. Petersen, T. M. Moran, and P. Palese.** 2010. Broadly protective monoclonal antibodies against H3 influenza viruses following sequential immunization with different hemagglutinins. PLoS Pathog. **6:**e1000796.
28. **Watanabe, T., S. Watanabe, T. Noda, Y. Fujii, and Y. Kawaoka.** 2003. Exploitation of nucleic acid packaging signals to generate a novel influenza virus-based vector stably expressing two foreign genes. J. Virol. **77:**10575–10583.
28a. **World Health Organization.** WHO manual on animal influenza diagnosis and surveillance. World Health Organization, Geneva, Switzerland. www.who.int.
29. **Wu, R., Y. Guan, Z. Yang, J. Chen, H. Wang, Q. Chen, Z. Sui, F. Fang, and Z. Chen.** 2009. A live bivalent influenza vaccine based on a H9N2 virus strain. Vaccine **28:**673–680.
30. **Yewdell, J. W., J. R. Bennink, G. L. Smith, and B. Moss.** 1985. Influenza A virus nucleoprotein is a major target antigen for cross-reactive anti-influenza A virus cytotoxic T lymphocytes. Proc. Natl. Acad. Sci. U. S. A. **82:**1785–1789.
31. **Zheng, H., P. Palese, and A. Garcia-Sastre.** 1996. Nonconserved nucleotides at the 3′ and 5′ ends of an influenza A virus RNA play an important role in viral RNA replication. Virology **217:**242–251.